Dalton Transactions

Accepted Manuscript

ROYAL SOCIETY OF CHEMISTRY

www.rsc.org/dalton

Cite this: DOI: 10.1039/c0xx00000x

www.rsc.org/xxxxxx

ARTICLE TYPE

A Highly Selective Phosphorescence Probe for Histidine in Living Bodies

Quankun Gao, Bo Song, Zhiqiang Ye,* Liu Yang, Ruoyang Liu, Jingli Yuan

Received (in XXX, XXX) Xth XXXXXXXXX 20XX, Accepted Xth XXXXXXXXX 20XX

DOI: 10.1039/b000000x

In this work, we designed and synthesized a heterobimetallic ruthenium(II)-nickel(II) complex, $[Ru(bpy)_2(phen\text{-}DPA)Ni](PF_6)_4$ (**Ru-Ni**), as a highly selective phosphorescence probe for histidine. The probe exhibited weak emission at 603 nm due to the phosphorescence of the Ru(II) complex can be strongly quenched by the paramagnetic Ni^{2+} ion. In the presence of histidine, reaction of **Ru-Ni** with histidine resulted in the release of nickel(II) and the enhancement in phosphorescence intensity at 603 nm. **Ru-Ni** showed high selectivity for histidine even in the presence of other amino acids and cellular abundant species. Cell imaging experimental results demonstrated that **Ru-Ni** is membrane permeable, and can be applied for visualizing histidine in live cells. More interestingly, **Ru-Ni** also can act as a novel reaction-based nuclear staining agent for visualizing exclusively the nuclei of living cells with a significant phosphorescence enhancement. In addition, the potential of the probe for biological applications was confirmed by employing it for phosphorescence imaging of histidine in larval zebrafish and *Daphnia magna.* These results demonstrated that **Ru-Ni** would be a useful tool for the physiological and pathological studies involved in histidine.

Introduction

Histidine (His) is an essential amino acid required for human growth.[1] It plays vital roles in biological systems such as serving as a neurotransmitter[2] and as a regulator of metal transmission.[3] A deficiency of histidine may result in the impaired nutritional state of patients with chronic kidney disease,[4] whereas excessive histidine may cause stress and psychological disorders.[5] Moreover, an abnormal level of histidine-rich proteins in the biological system could indicate a variety of diseases such as asthma and advanced liver cirrhosis.[6] Therefore, the accurate detection and quantification of histidine is an important goal for both biochemical and clinical applications. Several methods have been developed for the detection of histidine, such as capillary electrophoresis,[7-9] liquid chromatography,[10,11] voltammetry,[12] spectrophotometry,[13,14] mass spectrometry,[15] and resonance light scattering technique.[16] However, these methods are destructive and time-consuming, requiring homogenization of samples, which renders them unsuitable for detecting histidine in live cells and tissues.

Luminescent imaging, combining luminescent probes and an appropriate imaging instrument, is a promising tool for the nondestructive detection of targeted biomolecules with high sensitivity and spatial resolution.[17,18] However, so far only a few luminescent probes for histidine were reported.[19-27] A major challenge in achieving reliable histidine sensing is to design and synthesize small molecule-based luminescent probes that can selectively respond to histidine over other amino acids, especially in complicated biological systems. Recently, several copper (II)-indicator ensemble-based complexes were applied for histidine detection.[19-22] However, due to the high binding affinity of Cu (II) to sulfide, these probes suffered clear interference from cellular biothiols, such as cysteine (Cys, about 100 μM), reduced glutathione (GSH, in mM concentrations), and thio-containing proteins, which makes these probes be difficultly used for imaging histidine in live systems. Li et al. have reported an iridium(III)-solvent complex to afford turn-on fluorescence response to histidine.[26] However, it acts only as a nuclear imaging agent of live cells because proteins (such as BSA) also can induce the enhancement in phosphorescence of the solvent complex. Lack of luminescent probes for accurate detection of histidine in biological systems has hampered mechanistic researches on histidine generation and metabolization, and related diseases.

Here we report the development of a heterobimetallic ruthenium(II)-nickel(II) complex for highly sensitive and selective detection of histidine in aqueous solutions without the interference of other amino acids and cellular biothiols. In addition, the probe could be easily transferred into the cultured cells with the ordinary co-incubation method, and be applied for

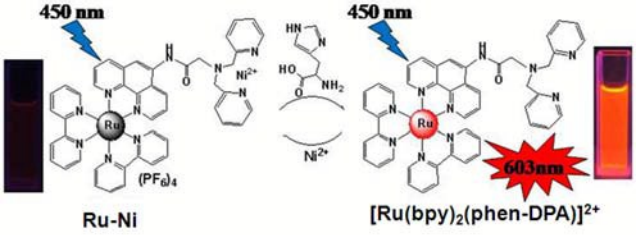

Scheme 1. Phosphorescence response mechanism of **Ru-Ni** to histidine.

determination of histidine in living cells, larval zebrafish and *Daphnia magna*. A phosphorescence bioimaging technique has been successfully developed for mapping histidine in complicated biological samples.

Experimental details

Materials and physical measurements

HeLa cells were obtained from Dalian Medical University. The PBS buffer consisting of 137 mM NaCl, 2.7 mM KCl , 10.1 mM Na_2HPO_4 and 1.8 mM KH_2PO_4 was prepared in our laboratory. Cultured *Daphnia magna* were obtained from School of Environmental Science and Technology, Dalian University of Technology. $Ru(bpy)_2(phen\text{-}Br)(PF_6)_2$ was synthesized according to the previously reported methods.[28] The solvents DMF and CH_3CN were used after appropriate distillation and purification. Hoechst 33342 was purchased from Aladdin. Unless otherwise stated, all chemical materials were purchased from commercial sources and used without further purification.

^1H and ^{13}C NMR spectra were measured on a Bruker Avance spectrometer (400 MHz for ^1H and 100 MHz for ^{13}C). Mass spectra were recorded on a HP1100 LC/MSD MS spectrometer. Elemental analysis was carried out on a Vario-EL analyser. Absorption spectra were measured on a Perkin-Elmer Lambda 35 UV-vis spectrometer. Emission lifetimes were measured on a steady/transient fluorescence spectrometer FLS 920 (Edinburgh Instruments). Phosphorescence spectra were measured on a Perkin-Elmer LS 50B fluorescence spectrometer with excitation and emission slits of 10 nm. Relative phosphorescence quantum yields of the complexes were measured with $Ru(bpy)_3Cl_2$ as the reference (ϕ = 2.8% in water).[29] All bright-field and phosphorescence imaging measurements were carried out on a Nikon TE 2000-E fluorescence microscope. The microscope, equipped with a 100 W mercury lamp, a Nikon B-2A filters and a colour CCD camera system (RET-2000R- F- CLR-12-C, Qimaging Ltd.), was used for phosphorescence imaging measurements. Exposure time: 8 s for HeLa cells, 2 s for zebrafish, and 1 s for *Daphnia magna*, respectively.

Syntheses of the complexes

The reaction pathway for the synthesis of $[Ru(bpy)_2(phen\text{-}DPA)](PF_6)_2$ and $[Ru(bpy)_2(phen\text{-}DPA)Ni](PF_6)_4$ (**Ru-Ni**) is shown in Scheme 2. The experimental details are described as follows.

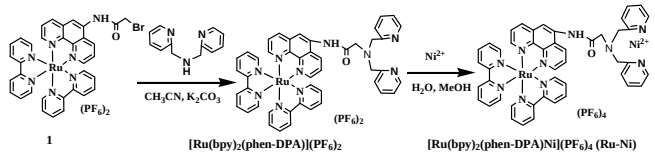

Scheme 2. Synthesis procedure of the Ru(II) complexes.

Syntheses of $[Ru(bpy)_2(phen\text{-}DPA)](PF_6)_2$

Compound 1 (207 mg, 0.2 mmol) was dissolved in 20 mL anhydrous CH_3CN, and then di(2-picolyl)amine (40 mg, 0.2 mmol) and anhydrous K_2CO_3 (166 mg, 1.2 mmol) were added into the solution. The mixture was refluxed with stirring for 24 h under an argon atmosphere. After filtration, the solvent was evaporated. The residue was purified by silica gel column chromatography using CH_3CN:KNO_3(sat.) =15:1 (v/v) as eluent. The fractions containing the target product were collected, and the solvent was evaporated. The resulting solid was dissolved in CH_3CN to remove the excess KNO_3 by filtration. After evaporation, the product $[Ru(bpy)_2(phen\text{-}DPA)](NO_3)_2$ was dissolved in a small amount (~5mL) of deionized distilled water, and a saturated aqueous solution of NH_4PF_6 was added to give a red precipitate. The precipitate was filtered, washed with water, and dried. $[Ru(bpy)_2(phen\text{-}DPA)](PF_6)_2$ was obtained as a red solid (107 mg, 47 % yield). ^1H NMR (400 MHz, CD_3CN): δ (ppm) = 11.84 (s, 1H), 9.39 (d, J = 8.0Hz, 1H), 8.90 (s, 1H), 8.55-8.49 (m, 5H), 8.39 (d, J = 4.0Hz, 2H), 8.18 (d, J = 5.0Hz, 1H), 8.13-8.07 (m, 2H), 8.02-7.95 (m, 3H), 7.90-7.86 (m, 2H), 7.83 (d, J = 6.0Hz, 1H), 7.69-7.64 (m, 3H), 7.60-7.54 (m, 2H), 7.48-7.42 (m, 2H), 7.36 (d, J = 8.0Hz, 2H), 7.26-7.22(m, 2H), 7.19 (t, J = 6.0Hz, 2H), 4.05 (s, 4H), 3.64 (s, 2H). ^{13}C NMR (CD_3CN): δ (ppm) = 170.9, 157.8, 157.0, 156.7, 152.2, 151.7, 151.6, 150.6, 149.0, 147.7, 144.5, 137.6, 137.5, 137.4, 136.7, 135.9, 133.9, 131.8, 130.9, 127.3, 127.2, 127.1, 125.8, 125.7,125.3, 123.9, 123.8, 123.4, 122.3, 117.0, 115.3, 59.8, 58.5. ESI-MS (m/z): 993.2 $[M\text{-}PF_6]^+$, 424.2 $[M\text{-}2PF_6]^{2+}$. Elemental analysis (%) calcd. for $C_{46}H_{36}F_{12}N_{10}OP_2Ru{\cdot}3H_2O$: C 46.35, H 3.72, N 11.75; found: C 46.62, H 3.36, N 11.56.

Syntheses of $[Ru(bpy)_2(phen\text{-}DPA)Ni](PF_6)_4$ (Ru-Ni)

$[Ru(bpy)_2(phen\text{-}DPA)](PF_6)_2$ (22.76 mg, 0.02 mmol) was dissolved in 5 mL MeOH. After a solution of $NiCl_2{\cdot}6H_2O$ (23.77 mg, 0.1 mmol) in 5 mL water was added dropwise. The mixture was stirred for 2 h at room temperature. The solvent was evaporated. The product was dissolved in a small amount (~5mL) of deionized distilled water, and a saturated aqueous solution of NH_4PF_6 was added. The precipitate was filtered, washed with water, and dried. **Ru-Ni** was obtained as an orange solid (27 mg, 90% yield). ESI-MS (m/z): 526.1 $[M\text{-}3PF_6{+}H]^{2+}$. Elemental analysis (%) calcd. for $C_{46}H_{38}F_{24}N_{10}OP_4NiRu$: C 37.17, H 2.58, N 9.42; found: C 37.14, H 2.88, N 9.61.

Phosphorescence imaging of histidine in live cells

HeLa cells were cultured in RPMI-1640 medium (Sigma-Aldrich, Inc.), supplemented with 10% fetal bovine serum (Corning Incorporated), 1% penicillin (Gibco), and 1% streptomycin (Gibco) at 37 °C in a 5% CO_2/95% air incubator. A 0.05 M PBS buffer solution of pH 7.4 (containing 0.5% DMSO as a co-solvent) containing 50 μM of **Ru-Ni** was prepared. The cultured HeLa cells in a glass bottom cell culture dish (ϕ = 20 mm) were washed with the PBS buffer, and then incubated with 2 mL of the above **Ru-Ni** solution. After incubation for 2 h at 37 °C in a 5% CO_2/95% air incubator, and then further incubated with PBS buffer solution containing Hoechst 33342 for 30 min, the cells were washed three times with PBS buffer, and then subjected to the phosphorescence imaging measurements.

MTT Assay

HeLa cells were cultured in RPMI-1640 medium (Sigma-Aldrich, Inc.), supplemented with 10% fetal bovine serum (Corning Incorporated), 1% penicillin (Gibco), and 1% streptomycin (Gibco) at a density of 10^5 cells/mL in a tissue culture plate. After **Ru-Ni** (final concentration: 0, 50, 100, 150, 200 μM) was added to the medium, the cells were incubated at 37 °C in a 5% CO_2/95% air incubator for 3 h, and then the culture medium was removed. The cells were further incubated in the culture medium containing 833 μg/mL of 3-(4,5-dimethyl- 2-thiazoyl)-2,5-diphenyltetrazolium bromide (MTT, Sigma) for 4 h. After supernatant was removed, the cells were dissolved in 80 μL DMSO, and then the absorbance at 540 nm was measured in an Infinite M200 Pro Microplate Reader.

Phosphorescence imaging of histidine in zebrafish

Zebrafish (Huante biological technology Co. Ltd. Hangzhou, China) were raised in nonchlorinated tap water at 28 °C and maintained at optimal breeding conditions. For mating, male and female zebrafish were maintained in one tank at 28 °C on a 12-h light/12-h dark cycle, and then the spawning of eggs was triggered by giving light stimulation in the morning. Almost all eggs were fertilized immediately. The 3-day-old zebrafish were maintained in E3 embryo media (containing 15 mM NaCl, 0.5 mM KCl, 1 mM $MgSO_4$, 1 mM $CaCl_2$, 0.15 mM KH_2PO_4, 0.05 mM Na_2HPO_4, 0.7 mM $NaHCO_3$, and 10^{-5}% methylene blue; pH 7.5).[30] The zebrafish were incubated with 50 μM **Ru-Ni** in E3 media for 2 h at 28 °C. After washing with PBS buffer to remove the remained probe, the zebrafish were subjected to the phosphorescence imaging measurements.

Phosphorescence imaging of histidine in *Daphnia magna*

Daphnia magna were raised in nonchlorinated tap water at 20°C under a cool-white fluorescent light with a 14:10 h light:dark photoperiod. The culture medium was renewed three times a week. Scenedesmusobliquus were fed to Daphnia magna daily. The newborn Daphnia magna (age < 48 h) were incubated with **Ru-Ni** (30 μM) in the culture medium for 2 h at 25 °C, washed four times with culture medium, and then subjected to the phosphorescence imaging measurements.

Results and discussion

Design, synthesis and photophysical properties of heterobimetallic Ru(II)–Ni(II) complexes

In this work, the novel heterobimetallic ruthenium(II)-nickel(II) complex was designed by incorporating a chelator-Ni(II) complex into a luminescent Ru(II)-bipyridine complex. The luminescent Ru(II) complex is a common platform in the design of imaging agents because of its outstanding photochemical and photophysical properties, such as intense visible excitation and emission, large Stokes shift, high photo- and thermal stabilities, and very low cytotoxicity.[31] After conjugated with a nickel(II) complex, the phosphorescence of the Ru(II) complex can be strongly quenched by the paramagnetic Ni^{2+} ion. At the same time, it is well known that nickel(II) has high binding affinity to histidine,[32,33] and some Ni^{2+}-chelates, such as Ni^{2+}-iminodiacetate (Ni-IDA) and Ni^{2+}-nitrilotriacetate (Ni-NTA), can bind the polyhistidine-tag at micromolar concentration. Therefore, we expected that Ni^{2+} could be released from the appropriate nickel(II) complex in the presence of histidine, to result in phosphorescence enhancement of the Ru(II) complex. Moreover, in comparison with Cu (II), Ni(II) shows much lower affinity to sulfide, which makes Ni(II) containing complexes be suitable for the highly selective recognition of histidine in live systems. On the basis of this hypothesis, we designed and synthesized a sensing probe based on a Ru(II) complex conjugated with Ni^{2+} complexes, employing dipicolylamine (DPA), as a chelator for Ni^{2+}. $[Ru(bpy)_2(phen\text{-}DPA)](PF_6)_2$ was well confirmed by NMR spectroscopy, ESI-MS and elemental analyses (Fig. S1-S4 in Electronic Supplementary Information).

The phosphorescence properties of the Ru(II) complexes were shown in Table S1 of Electronic Supplementary Information. UV-vis absorption spectra of the Ru(II) complexes exhibited intense absorption peaks at 450 nm (Fig. S6), which is attributed to the typical metal-to-ligand charge transfer (MLCT) transition of the ruthenium(II)-diimine complexes. Though the phosphorescence lifetimes (> 600 ns, Fig. S7) were not affected by the Ni^{2+} binding, the **Ru-Ni** complex is weakly luminescent with the low phosphorescence quantum yield, indicating that Ni^{2+} can effectively quench the phosphorescence of the Ru(II) complex as we expected. Next, we examined the phosphorescence response of the Ru(II)–Ni(II) complexes to histidine. In the presence of histidine, **Ru-Ni** showed excellent phosphorescence response to histidine, and its phosphorescence intensity was remarkably increased with up to 11-fold enhancement. The mass spectrum of the product of **Ru-Ni** reacted with histidine confirmed the generation of the complex $[Ru(bpy)_2(phen\text{-}DPA)](PF_6)_2$ (the MS signals at m/z 424.2 and 993.1, Fig. S5) accompanied by the release of Ni^{2+} from the Ru(II)–Ni(II) complex. This result demonstrated that **Ru-Ni** could act as a phosphorescence sensing probe for histidine.

Phosphorescence Response of Ru-Ni to histidine

To investigate the feasibility of **Ru-Ni** as a phosphorescence probe for the quantitative detection of histidine, the excitation and emission spectra of **Ru-Ni** in the presence of different concentrations of histidine were recorded in EtOH/HEPES buffer

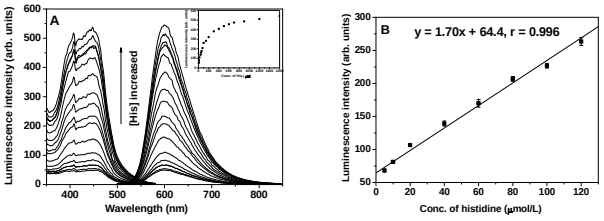

Fig. 1. A: Excitation and emission spectra of Ru-Ni (10 μM) in the presence of different concentrations of histidine (0.0, 1.0, 5.0, 10, 20, 50, 80, 100, 150, 200, 300, 500, 700, 900, 1200 and 1600 μM) in EtOH/HEPES buffer (50 mM, pH 7.2, 2 : 3, v/v). The inset shows the emission intensity change of Ru-Ni at 603 nm in the presence of different concentrations of histidine. B: Calibration curve for histidine detection (0-120 μM).

(50 mM, pH 7.2, 2:3, v/v). As shown in Fig. 1A, the emission at 603 nm of **Ru-Ni** was increased upon addition of histidine. The dose-dependent phosphorescence enhancement showed a good linearity in the histidine concentration range of 5-120 μM (Fig. 1B). The detection limit for histidine, calculated according to the reported method defined by IUPAC,[34, 35] is 265 nM, suggesting that **Ru-Ni** could be used as a highly sensitive phosphorescence probe for histidine.

Next, we evaluated the response specificity of the probe towards histidine. The phosphorescence responses of **Ru-Ni** to various amino acids and several cellular abundant species were examined in EtOH/HEPES buffer (50 mM, pH 7.2, 2:3, v/v). As shown in Fig. 2A, **Ru-Ni** showed high response selectivity towards histidine over biothiols, such as cysteine, GSH, and homocysteine. Various anions (Fig. 2B), ascorbic acid, DNA, BSA, and other amino acids (including proline (Pro), tyrosine (Tyr), glutamic acid (Glu), arginine (Arg), serine (Ser), leucine(Leu), tryptophan (Trp), valine (Val), alanine (Ala), glycine (Gly), threonine (Thr), aspartic acid (Asp)) could not induce observable changes on the emission intensity of **Ru-Ni**. In addition, the competition experiment results shown in Fig. 2 proved that the co-existence of other species did not affect the phosphorescence response of the probe to histidine. All of these results suggested that **Ru-Ni** could be a useful probe for the highly selective detection of histidine even in complicated cellular milieu.

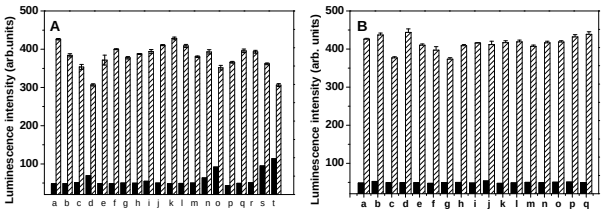

Fig. 2. A: Phosphorescence intensities (603 nm) of **Ru-Ni** (10 μM) after reaction with bioactive species (500 μM, black bars) in the absence and presence of histidine (500 μM, sparse bars) in EtOH/HEPES buffer (50 mM, pH 7.2, 2 : 3, v/v). a: blank; b: Pro; c: Tyr; d: GSH; e: Glu; f: Arg; g: Ser; h: Leu; i: Trp; j: Val; k: Ala; l: Gly; m: Thr; n: Hcy; o: Cys; p: Vc; q: cysteamine; r: calf thymus DNA; s: Asp; t: BSA (1 %). B: Phosphorescence intensities (603 nm) of **Ru-Ni** (10 μM) after reaction with different anions (500 μM, black bars) in the absence and presence of histidine (500 μM, sparse bars) in EtOH/HEPES buffer (50 mM, pH 7.2, 2 : 3, v/v). a: blank; b: Br^-; c: $S_2O_3^{2-}$; d: HPO_4^{2-}; e: Cl^-; f: MoO_4^{2-}; g: ClO^-; h: $S_2O_5^{2-}$;i: SO_4^{2-}; j: CO_3^{2-}; k: F^-; l: AcO^-; m: HSO_3^-; n: $H_2PO_4^-$; o: I^-; p: HCO_3^-; q: NO_3^-.

Phosphorescence Imaging of Histidine in Living Cells

The photophysical properties of **Ru-Ni**, such as large Stokes shifts and excellent photostability, as well as its selectivity for histidine, seemed appropriate for cellular use, so we examined the practical utility of **Ru-Ni** for phosphorescence imaging of cellular histidine. At first, we examined the cytotoxicity of **Ru-Ni** by using the MTT assay method. No significant differences in the proliferation of HeLa cells were observed in the absence and presence of **Ru-Ni** (Fig. S9), demonstrating that the toxicity of **Ru-Ni** to HeLa cells is negligible. After HeLa cells were incubated with **Ru-Ni** (50 μM) for 2 h at 37 °C, clearly red phosphorescence was detected in the nuclear region, while the phosphorescence in the cytoplasm was very weak (Fig. 3A). As shown in Fig. 3b-H, quantification of the phosphorescence intensity profile of **Ru-Ni**–loaded cells revealed a high signal ratio (~60-fold) between the nucleus and the cytoplasm, which indicates that histidine and histidine-containing proteins mainly locate in the nuclear region of the cells. In addition, the **Ru-Ni**–loaded HeLa cells were co-incubated the dye Hoechst 33342 (a commercial nuclear imaging agent). As shown in Fig. 3b, a red spot, the phosphorescence of **Ru-Ni**, perfectly colocalized with a blue spot obtained at the filter setting for Hoechst 33342, and the colocalization was evident from a bright pink spot in the region of the nucleus. This fact indicates that **Ru-Ni** also can act as a phosphorescence-enhanced imaging agent for cell nuclei.

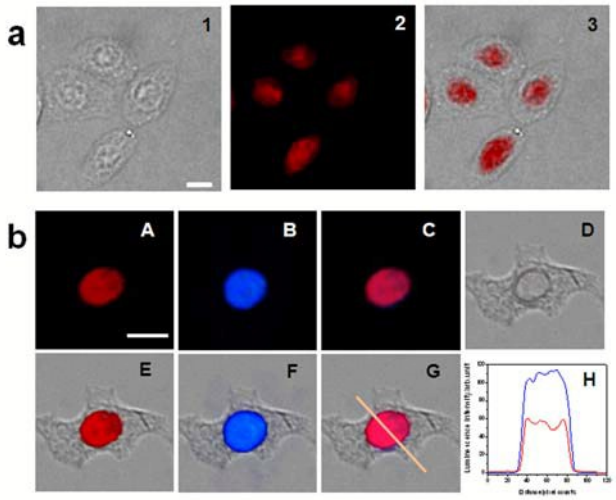

Fig. 3.a: Phosphorescence images of HeLa cells incubated with **Ru-Ni** (50 μM) for 2 h at 37 °C. 1: Bright-field image; 2: phosphorescence image (excitation filter, 450-490 nm; dichroic mirror, 505 nm; emission filter, > 590 nm); 3: overlay of 1 and 2. **b**: Phosphorescence images of HeLa cells incubated with **Ru-Ni** for 2 h and then further incubated with Hoechst 33342 (200 nM) for 30 min at 37 °C. A: Phosphorescence images derived from **Ru-Ni** (excitation filter, 450-490 nm; dichroic mirror, 505 nm; emission filter, > 590 nm); B: phosphorescence images derived from Hoechst 33342 (excitation filter, 330-380 nm; dichroic mirror, 400 nm; emission filter, >420 nm); C: overlay of A and B; D: bright-field image; E: overlay of A and D; F: overlay of B and D; G: overlay of C and D; H: phosphorescence intensity profiles of **Ru-Ni** (red line) and Hoechst 33342 (blue line) in the interest linear region across a HeLa cell. Image analysis was performed using Image J software. Scale bar: 10 μm.

Phosphorescence Imaging of Histidine in Living bodies

To explore the potential of the probe as an in vivo imaging tool, **Ru-Ni** was applied to histidine detection in live larval zebrafish. We first tested the toxicity of **Ru-Ni** in larval zebrafish. After 20 h incubation in E3 embryo media containing 50 μM **Ru-Ni,** no significant toxicity to larval zebrafish was observed, suggesting the safe use of **Ru-Ni** as a viable in vivo phosphorescence reporter over the time scale of hours. After incubated with **Ru-Ni** for 2 h, 3-day-old zebrafish showed strongly red phosphorescence signals mainly in the range of abdomen (Fig. 4A). In addition, a control experiment was carried out by treating zebrafish with 50

μM of **Ru-Ni** for 2 h, followed by the incubation with Ni^{2+} for 1 h. In this case, only very weak red phosphorescence could be observed from zebrafish (Fig. 4B), demonstrating that the red phosphorescence signals in larval zebrafish were indeed originated from the reaction of **Ru-Ni** with endogenous histidine. These results suggest that **Ru-Ni** can efficiently penetrate tissues, and has potential utility in detecting histidine in vivo.

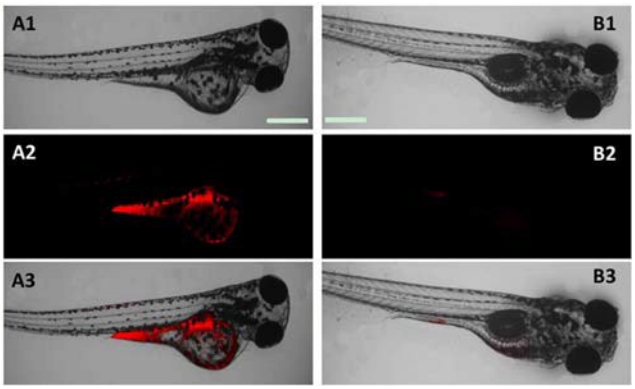

Fig. 4. Phosphorescence images of zebrafish incubated with **Ru-Ni**. A1-A3: Bright-field, phosphorescence and merged images of zebrafish incubated with **Ru-Ni**. (50 μM) for 2 h at 28 °C. B1-B3: Bright-field, phosphorescence and merged images of zebrafish pre-treated with **Ru-Ni** (50 μM) for 2 h and then incubated with Ni^{2+} (50 μM) for 1 h at 28 °C. Scale bar: 500 μm.

Finally, we investigated the utility of **Ru-Ni** for phosphorescence imaging of histidine in living *Daphnia magna*, a widely used laboratory animal as a indicator of aquatic ecosystem health and as a model animal in ecotoxicology.[36, 37] As shown in Fig. 5, after incubated with **Ru-Ni**, *Daphnia magna* showed strongly red phosphorescence signals mainly in the range of esophagus, midgut and hindgut, which revealed that the probe molecules were transferred into the body of *Daphnia magna* through their food process, and then reacted with histidine distributed in the digestive system to give the red phosphorescence signals.

Fig. 5. Bright-field (A), phosphorescence (B) and merged (C) images of *Daphnia magna* that incubated with **Ru-Ni** (30 μM) for 2 h at 25 °C. Scale bar: 200 μm.

Conclusions

In this work, we designed and synthesized a novel heterobimetallic Ru(II)-Ni(II) complex, **Ru-Ni,** for the recognition and phosphorescence detection of histidine in live samples. This probe possesses several advantageous photophysical properties, such as visible-light absorption and emission, long-lived excited state, and large Stokes shift (153 nm), which enables the self-quenching of phosphorescence to be effectively avoided. **Ru-Ni** showed satisfactory applicability for the detection of histidine under physiological conditions with high selectivity and sensitivity. In addition, the low-toxicity of the probe allowed it to be used for the monitoring of endogenous histidine in HeLa cells and living bodies. We anticipate that **Ru-Ni** could be a useful tool for the investigation of a wide range of biological functions of histidine in physiological disease and ecotoxicology.

Acknowledgements

Financial support from the National Natural Science Foundation of China (Grant No. 21475015) is gratefully acknowledged.

Notes and references

State Key Laboratory of Fine Chemicals, School of Chemistry, Dalian University of Technology, Dalian 116024, China. Fax: +86-411-84986042; Tel: +86-411-84986042; E-mail: yezq@dlut.edu.cn

†Electronic Supplementary Information (ESI) available: photophysical parameters, and decay traces of the Ru(II) complexes, cytotoxicity measurements, and the supplementary Figures. See DOI: 10.1039/b000000x/

1 F. Zhao, E. Ghezzo-Schöneich, G. I. Aced, J. Hong, T. Milby and C. Schöneich, *J. Biol. Chem.*, 1997, **272,** 9019.
2 Y. Bessho, E. Iwakoshi-Ukena, T. Tachibana, S. Maejima, S. Taniuchi, K. Masuda, K. Shikano, K. Kondo, M. Furumitsu and K. Ukena, *Neurosci. Lett.*, 2014, **578**, 106.
3 G. N. Chen, X. P. Wu, J. P. Duan and H. Q. Chen, *Talanta,* 1999, **49**, 319.
4 M. Watanabe, M. E. Suliman, A. R. Qureshi, E. Garcia-Lopez, P. Bárány, O. Heimbürger, P. Stenvinkel and B. Lindholm, *Am. J. Clin. Nutr.*, 2008, **87**, 1860.
5 L. Jones, M. D. Hulett and C. R. Parish, Immunol. *Cell Biol.*, 2005, **83,** 106.
6 F. W. Leebeek, C. Kluft, E. A. Knot and M. P. De Matt, *J. Lab. Clin. Med.*, 1989, **113,** 493.
7 L. Zhou, N. Yan, H. Zhang, X. Zhou, Q. Pu and Z. Hu, *Talanta,* 2010, **82,** 72.
8 L. -Y. Zhang and M. -X. Sun, *J. Chromatogr. A.*, 2004, **1040,** 133.
9 J. Meng, W. Zhang, C. -X. Cao, L. -Y. Fan, J. Wu and Q. -L. Wang, *Analyst,* 2010, **135,** 1592.
10 N. Tateda, K. Matsuhisa, K. Hasebe and T. Miura, *Anal. Sci.,* 2001, **17,** 775.
11 S. Wadud, M. M. Or-Rashid and R. Onodera, *J. Chromatogr. B.,* 2002, **767,** 369.
12 M. Shahlaei, M. B. Gholivand and A. Pourhossein, *Electroanalysis,* 2009, **21,** 2499.
13 L. Fabbrizzi, P. Pallavicini, L. Parodi, A. Perotti and A. Taglietti, *J. Chem. Soc., Chem. Commun.,* 1995, **23,** 2439.
14 J. D. Swartz, C. P. Gulka, F. R. Haselton and D. W. Wright, *Langmuir,* 2011, **27,** 15330.
15 T. Furuta, M. Katayama, H. Shibasaki and Y. Kasuya, *J. Chromatogr. B Biomed.Sci. Appl.,* 1992, **576,** 213.
16 Z. Chen, J. Liu, Y. Han and L. Zhu, *Anal. Chim.Acta.,* 2006, **570,** 109.
17 Q. Zhao, C. Huang and F. Li, *Chem. Soc. Rev.*, 2011, **40,** 2508.
18 Y. Yang, Q. Zhao, W. Feng and F. Li, *Chem. Rev.*, 2013, **113,**192.
19 Q. -H. You, A. W.-M.Lee, W.-H.Chan, X.-M. Zhu and K. C.-F. Leung, *Chem. Commun.*, 2014, **50,** 6207.
20 B. Wang, Y. Gao, H.-W. Li, Z.-P. Hu and Y. Wu, *Org. Biomol. Chem.*, 2011, **9,** 4032.
21 F. Pu, Z. Huang, J. Ren and X. Qu, *Anal. Chem.*, 2010, **82,** 8211.
22 H.-Z. He, M. Wang, D. S.-H.Chan, C.-H.Leung, J.-W.Qiu and D.-L. Ma, *Methods,* 2013, **64,** 205.
23 M. A. Hortalá, L. Fabbrizzi, N. Marcotte, F. Stomeo and A. Taglietti, *J. Am. Chem. Soc.,* 2003, **125,** 20.

24 D.-L. Ma, W.-L.Wong, W.-H.Chung, F.-Y.Chan, P.-K.So, T.-S.Lai, Z.-Y.Zhou, Y.-C.Leung and K.-Y. Wong, *Angew. Chem. Int. Ed.,* 2008, **47,** 3735.

25 Z. Huang, J. Du, J. Zhang, X.-Q.Yu and L. Pu, *Chem. Commun.,* 2012, **48,** 3412.

26 C. Li, M. Yu, Y. Sun, Y. Wu, C. Huang and F. Li, *J. Am. Chem. Soc.,* 2011, **133,** 11231.

27 X. Wang, J. Jia, Z. Huang, M. Zhou and H. Fei, *Chem. Eur. J.,* 2011, **17,** 8028.

28 Z. Ye, X. An, B. Song, W. Zhang, Z. Dai and J. Yuan, *Dalton Trans.*, 2014, **43,** 13055.

29 A. Juris and V. Balzani, *Coord. Chem. Rev.,* 1988, **84,** 85.

30 L. A. Greene and A. S. Tischler, *Proc. Natl. Acad. Sci. USA.,* 1976, **73,** 2424.

31 K. K.-W. Lo, T. K.-M. Lee, J. S.-Y. Lau, W.-L.Poon and S.-H. Cheng, *Inorg. Chem.,* 2008, **47,** 200.

32 Y. Hu, Q. Wang, C. Zheng, L. Wu, X. Hou and Y. Lv, *Anal. Chem.,* 2014, **86,** 842.

33 P. Wu and X.-P. Yan, *Biosens. Bioelectron.,* 2010, **26,** 485.

34 J. Mocak, A. M. Bond, S. Mitchell and G. Scollary, *Pure. Appl. Chem.,* 1997, **69,** 297.

35 V. Thomsen, D. Schatzlein and D. Mercuro, *Spectroscopy,* 2003, **18,** 112.

36 M. Heinlaan, A. Lvaska, I. Blinovaa, H. Dubourguierb and A. Kahrua, *Chemosphere,* 2008, **71,** 1308.

37 S. B. Lovern and R. Klaper, *Environ. Toxicol.Chem.,* 2006, **25,** 1132.

Graphical contents entry

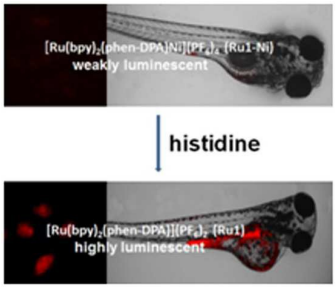

A heterobimetallic ruthenium(II)-nickel(II) complex has been developed for phosphorescence imaging of histidine in live cells and bodies..